Published on 25 September 2014. Downloaded by UNIVERSIDAD ESTADUAL DE CAMPINAS on 26/06/2015 20:14:22.

PCCP

PAPER

View Article Online
View Journal | View Issue

Cite this: *Phys. Chem. Chem. Phys.*, 2014, **16**, 23224

Atomic charge transfer-counter polarization effects determine infrared CH intensities of hydrocarbons: a quantum theory of atoms in molecules model†

Arnaldo F. Silva, Wagner E. Richter, Helen G. C. Meneses and Roy E. Bruns*

Atomic charge transfer-counter polarization effects determine most of the infrared fundamental CH intensities of simple hydrocarbons, methane, ethylene, ethane, propyne, cyclopropane and allene. The quantum theory of atoms in molecules/charge–charge flux–dipole flux model predicted the values of 30 CH intensities ranging from 0 to 123 km mol^{-1} with a root mean square (rms) error of only 4.2 km mol^{-1} without including a specific equilibrium atomic charge term. Sums of the contributions from terms involving charge flux and/or dipole flux averaged 20.3 km mol^{-1}, about ten times larger than the average charge contribution of 2.0 km mol^{-1}. The only notable exceptions are the CH stretching and bending intensities of acetylene and two of the propyne vibrations for hydrogens bound to sp hybridized carbon atoms. Calculations were carried out at four quantum levels, MP2/6-311++G(3d,3p), MP2/cc-pVTZ, QCISD/6-311++G(3d,3p) and QCISD/cc-pVTZ. The results calculated at the QCISD level are the most accurate among the four with root mean square errors of 4.7 and 5.0 km mol^{-1} for the 6-311++G(3d,3p) and cc-pVTZ basis sets. These values are close to the estimated aggregate experimental error of the hydrocarbon intensities, 4.0 km mol^{-1}. The atomic charge transfer-counter polarization effect is much larger than the charge effect for the results of all four quantum levels. Charge transfer-counter polarization effects are expected to also be important in vibrations of more polar molecules for which equilibrium charge contributions can be large.

Received 3rd July 2014,
Accepted 11th September 2014

DOI: 10.1039/c4cp02922d

www.rsc.org/pccp

Introduction

Infrared vibrational intensities of the hydrocarbon molecules have been studied for many years since they are sensitive probes of molecular electronic structure changes during vibrations. One of the goals of these investigations has been the determination of hydrogen equilibrium atomic charges. Experimental intensity studies by King and collaborators[1] using the G intensity sum rule showed that the hydrogen atom charges in C_2H_2 and HCN are significantly more positive than those of the other simple hydrocarbons in line with their known acidic properties. Electrooptical and equilibrium charge–charge flux (ECCF) models contemplating equilibrium atomic charges and their changes upon vibration have been used to interpret the infrared fundamental intensities.[2–5] Owing to symmetry out-of-plane vibrations do not have charge rearrangements upon vibration and the ECCF model was used to determine atomic charges completely from experimental structure and spectral data.[6–8] Applications treating molecular orbital results included a quantum mechanical interference term embedded in a charge–charge flux–overlap (CCFO) model.[9]

Warnings have been issued that electronic structure models should not ignore the dipolar relaxations of the charge density that are an essential characteristic of vibrational displacements.[10] Bearing this in mind the quantum theory of atoms in molecules (QTAIM)[11,12]/charge–charge flux–dipole flux (CCFDF)[13,14] model has been applied here to a group of small hydrocarbons to determine the importance of static and dynamic contributions to their CH stretching and deformation vibrational intensities. Charge flux contributions result from intramolecular charge transfer and have been considered in most of the models mentioned above. However the dipole flux contribution includes changes in the polarization of the atomic dipoles during the molecular vibrations and is not included in the above models.

The difficulties in measuring accurate gas phase infrared intensities[15,16] are well known and care must be taken in choosing the experimental intensity results to be used for comparison with the theoretical values. Furthermore, experimental intensities suffer from anharmonicity effects that are normally

Instituto de Química, Universidade Estadual de Campinas, CP 6154, 13084-970 Campinas, SP, Brazil. E-mail: bruns@iqm.unicamp.br

† Electronic supplementary information (ESI) available. See DOI: 10.1039/c4cp02922d

This journal is © the Owner Societies 2014

Published on 25 September 2014. Downloaded by UNIVERSIDAD ESTADUAL DE CAMPINAS on 26/06/2015 20:14:22.

not included in quantum chemical estimates. On the other hand, intensity measurements on isotopically substituted molecules have often been carried out to remove dipole moment derivative sign ambiguities and these can serve as an internal check on the consistency of the intensity results. In practice comparison of intensities for isotopomers is only useful when hydrogen is substituted by deuterium, so the hydrocarbon molecules are especially attractive for testing quantum chemical methods for accuracy in spite of anharmonicity concerns.

For some of the hydrocarbons more than a half-dozen different measurements have been made. Of course some of these are very early measurements and are not of the same quality as others that were measured later. For determining which experimental data should be included in our study three criteria had to be satisfied: (1) intensities must have been measured for all the fundamental bands of the molecule, (2) error estimates from scattering of Beer's law plots must have been reported and (3) intensity measurements and error estimates must have been made for at least two isotopomers. So the G intensity sum rule[17] and the isotopic invariance property of atomic polar tensor elements[18,19] can be applied to these data providing some validation of the experimental measurements.

In this work the theoretical calculation of infrared intensities of the hydrocarbon molecules are investigated at two electron correlation treatment levels, the Quadratic Configuration Interaction with Single and Double excitations (QCISD)[20] and the second order Møller–Plesset perturbation (MP2)[21] levels, and two commonly used basis sets, Dunning's cc-pVTZ set[22] and the 6-311++G(3d,3p) one.[23] The QCISD level and cc-pVTZ basis set were chosen based on our recent study involving eight molecules showing that QCISD/cc-pVTZ wave functions are preferable to a large number of alternatives when considering both accuracy of intensity results and computational demand.[24] Furthermore the MP2 level with the 6-311++G(3d,3p) basis has been frequently used by our group to calculate the intensities of a large variety of molecules.[16] Factorial design models were then determined to investigate the effects of changing these basis sets and electron correlation treatment levels.[25] Finally the most accurate wave function for calculating the intensities was used to obtain the QTAIM parameters and charge–charge flux–dipole flux models with the aim of understanding the physical phenomena underlying the infrared fundamental intensities of the simple hydrocarbons.

Experimental and theoretical intensities

Theoretical intensity values were calculated on an AMD 64 Opteron workstation using the Gaussian 03 program.[26] Molecular geometries were optimized at both electron correlation treatment levels, MP2 and QCISD, using both basis sets, 6-311++G(3d,3p) and cc-pVTZ levels and were used to calculate the intensities. QTAIM atomic charges and dipoles were calculated using the MORPHY98 program.[27] Charge and dipole flux contributions were calculated using the PLACZEK program[28] from atomic charges and dipoles calculated using MORPHY98 for atomic displacements of ±0.01 Å. The derivatives are averages of those calculated for positive and negative displacements.

The experimental intensity data used for comparison with the theoretical results follow the criteria stated in the Introduction. The selected experimental intensities and their error estimates are presented in Table 1. The methane data were taken from four different experimental studies,[29–31] the acetylene intensity values from three sets of determinations[32–34] and the ethylene[35,36] and methyl acetylene[37,38] intensities from two sources. The ethane,[39]

Table 1 Experimental fundamental frequencies, intensities and theoretical values calculated at the MP2 and QCISD levels with the 6-311++G(3d,3p) and cc-p-VTZ basis sets

			6-311++G(3d,3p)		cc-pVTZ		
	ν_i	A_i (exp)	MP2	QCISD	MP2	QCISD	Sum
CH_4							
Q_3	3019.0	67.5 ± 1.5	54.1	72.9	49.9	69.3	68.7
Q_4	1311.0	33.5 ± 0.8	30.9	29.3	34.6	30.0	33.0
C_2H_2							
Q_3	3282.0	70.2 ± 4.3	91.4	78.7	96.1	84.7	83.4
Q_5	730.0	177 ± 21	183.7	183.6	178.8	181.6	178.7
C_2H_4							
Q_7	949.2	82.1 ± 2.5	97.2	93.3	98.2	89.1	89.6
Q_9	3105.5	25.5 ± 1.8	15.2	21.8	14.4	20.7	21.0
Q_{10}	810.3	0.3 ± 0.0	0.0	0.0	0.1	0.0	0.1
Q_{11}	2989.5	13.9 ± 1.2	10.8	15.0	9.6	13.4	13.8
Q_{12}	1443.5	10.1 ± 0.2	8.3	7.5	8.8	8.6	8.0
C_2H_6							
Q_5	2915.0	47.8 ± 0.5	50.9	55.9	47.8	53.2	52.8
Q_6	1379.2	4.0 ± 0.4	0.7	0.3	1.3	0.8	0.9
Q_7	2995.5	123.2 ± 1.4	101.7	130.4	95.6	124.5	124.3
Q_8	1472.2	13.4 ± 0.2	16.7	15.9	16.9	14.7	16.1
Q_9	821.5	6.1 ± 0.1	6.0	4.6	6.6	5.3	5.2
C_3H_4 (prop.)							
Q_1	3334.0	44.2 ± 2.4	54.1	49.4	57.1	53.2	52.4
Q_2	2930.0	17.2 ± 3.2	14.6	17.1	9.0	15.3	11.5
Q_3	2142.0	5.3 ± 0.3	3.6	3.7	2.4	2.9	2.5
Q_4	1380.0	1.5[a]	0.2	0.6	0.1	0.2	0.2
Q_5	930.0	0.8 ± 0.4	0.7	1.1	0.6	0.9	1.0
Q_6	2981	16.6 ± 2.9	8.9	15.3	12.8	15.3	19.2
Q_7	1452.0	17.9[a]	16.3	14.5	15.6	14.3	13.8
Q_8	1052.0	0.3 ± 0.2	0.2	0.01	0.5	0.2	0.3
Q_9	633.0	87.9 ± 5.0	92.4	90.7	90.0	89.4	88.3
Q_{10}	327.0	16.2 ± 0.8	15.6	15.9	13.0	14.6	13.3
C_3H_6							
Q_6	3102.0	30.2 ± 2.5	18.6	31.0	29.4	27.9	41.8
Q_7	854.0	0.5	0.3	0.1	0.4	0.2	0.2
Q_8	3024.0	38.5 ± 2.4	30.8	43.8	16.5	41.3	29.5
Q_9	1438.0	1.8 ± 0.1	1.4	0.8	1.9	1.4	1.3
Q_{10}	1028.0	20.3 ± 0.3	20.7	13.3	21.8	15.3	14.4
Q_{11}	869.0	31.1 ± 0.6	38.0	39.2	37.9	39.5	39.1
C_3H_4 (allene)							
Q_5	3007.0	5.5 ± 0.8	0.3	2.5	0.1	2.3	2.3
Q_6	1957.0	47.8 ± 1.2	51.2	54.7	44.7	51.4	48.2
Q_7	1398.0	6.1 ± 1.3	2.5	1.7	3.3	2.5	2.5
Q_8	3085.0	3.5 ± 0.6	0.2	2.4	0.2	1.6	2.4
Q_9	999.0	8.6 ± 1.8	5.0	6.1	2.8	3.9	3.9
Q_{10}	841.0	91.6 ± 2.0	105.5	99.0	108.3	103.5	101.8
Q_{11}	356.0	19.9 ± 0.6	14.0	13.1	11.5	14.6	10.6

[a] Overlapped bands. The sum of the intensities is 19.3 ± 1.3 km mol^{-1}.

Published on 25 September 2014. Downloaded by UNIVERSIDAD ESTADUAL DE CAMPINAS on 26/06/2015 20:14:22.

allene[40] and cyclopropane[41] intensities were each measured at one laboratory.

Infrared fundamental intensities are proportional to the square of the dipole moment derivatives with respect to normal coordinates,[42]

$$A_k = \frac{N\pi}{3c^2}\left(\frac{\partial \vec{p}}{\partial Q_k}\right)^2 \quad k = 1, \ldots 3N-6. \tag{1}$$

These derivatives are the result of three contributions to the dipole moment derivative owing to charge, charge flux and dipole flux terms[13]

$$\begin{aligned}\frac{\partial p_\sigma}{\partial Q_k} &= \sum_i q_i \frac{\partial \sigma_i}{\partial Q_k} + \sum_i \frac{\partial q_i}{\partial Q_k}\sigma_i + \sum_i \frac{\partial m_{i,\sigma}}{\partial Q_k} \\ &= \left(\frac{\partial p_\sigma}{\partial Q_k}\right)_{\mathrm{C}} + \left(\frac{\partial p_\sigma}{\partial Q_k}\right)_{\mathrm{CF}} + \left(\frac{\partial p_\sigma}{\partial Q_k}\right)_{\mathrm{DF}}\end{aligned} \tag{2}$$

with $\sigma = x, y, z$, i being summed over all atoms in the molecule and q_i and $m_{i,\sigma}$ representing atomic charges and atomic dipole Cartesian components.

The CCFDF contributions[14] to the infrared intensity are given by

$$\begin{aligned}A_k = \left(\frac{N\pi}{3c^2}\right)\sum_\sigma \Bigg[&\left(\frac{\partial p_\sigma}{\partial Q_k}\right)_{\mathrm{C}}^2 + \left(\frac{\partial p_\sigma}{\partial Q_k}\right)_{\mathrm{CF}}^2 + \left(\frac{\partial p_\sigma}{\partial Q_k}\right)_{\mathrm{DF}}^2 \\ &+ 2\left(\frac{\partial p_\sigma}{\partial Q_k}\right)_{\mathrm{C}}\left(\frac{\partial p_\sigma}{\partial Q_k}\right)_{\mathrm{CF}} + 2\left(\frac{\partial p_\sigma}{\partial Q_k}\right)_{\mathrm{C}}\left(\frac{\partial p_\sigma}{\partial Q_k}\right)_{\mathrm{DF}} \\ &+ 2\left(\frac{\partial p_\sigma}{\partial Q_k}\right)_{\mathrm{CF}}\left(\frac{\partial p_\sigma}{\partial Q_k}\right)_{\mathrm{DF}}\Bigg]\end{aligned} \tag{3}$$

The first three squared terms represent the charge, charge flux and atomic dipole flux contributions to the kth fundamental vibrational intensity. The last three terms correspond to interactions between charge, charge flux and dipole flux contributions and can be positive when both derivative contributions are of the same sign, reinforcing the total intensity, or negative when the contributions have opposite signs, decreasing the total intensity.

Results

Table 1 contains the experimental fundamental intensity values and estimated errors for methane, acetylene, ethylene, ethane, propyne, cyclopropane and allene. Theoretical values are provided at the MP2 and QCISD levels calculated using both the 6-311++G(3d,3p) and cc-pVTZ basis sets. The theoretical results are graphed against the experimental values in Fig. 1. In most cases the QCISD values are closer to the line representing exact agreement than those calculated at the MP2 level. A tendency for the QCISD results to over-estimate the experimental values can be observed for intensity values above about 40 km mol^{-1}. This behavior was also observed in our previous MP2/6-311++G(3d,3p) study for the high intensity bands of a diverse group of thirty molecules.[43]

Table 2 contains the root mean square (rms) error values for each molecule and each quantum level and basis set combination.

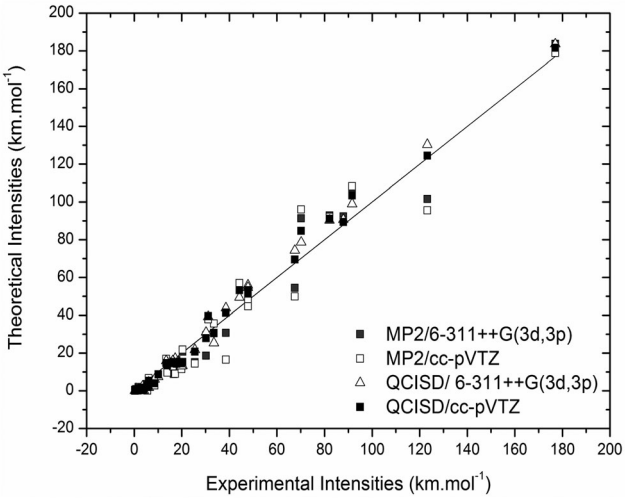

Fig. 1 Theoretical intensities obtained using two electron correlation treatment levels, MP2 and QCISD, and two basis sets, 6-311++G(3d,3p) and cc-pVTZ *vs.* the experimental values for the hydrocarbons.

Table 2 Root mean square errors (rms)[a] for the calculated intensities of each molecule for the four calculational levels (in km mol^{-1})

	MP2		QCISD		Exp.
Molecule	6-311++G(3d,3p)	cc-pVTZ	6-311++G(3d,3p)	cc-pVTZ	error
CH_4	9.5	12.5	7.5	2.5	1.2
C_2H_2	15.7	18.4	7.6	10.8	15.2
C_2H_4	6.9	7.0	4.3	4.6	1.5
C_2H_6	9.9	12.5	5.3	2.9	0.7
C_3H_4 (prop.)	4.4	5.3	2.3	3.3	2.5
C_3H_4 (allene)	6.5	7.9	5.1	5.7	1.3
C_3H_6	6.4	7.7	4.6	5.6	1.6
Total	7.6	9.1	4.7	5.0	4.0

[a] rms error = $\{\sum(y_{\mathrm{calc}} - y_{\mathrm{exp}})^2/n\}^{1/2}$, where n = the number of fundamental intensities of the molecules.

The total rms error given there shows that the QCISD level calculations are within about 5 km mol^{-1} of the experimental values. This is close to the averaged estimate of the experimental error for these molecules which is 4.0 km mol^{-1}. The MP2 rms errors are about twice this experimental uncertainty.

Two level factorial design[44] calculations performed on the results of Table 1 quantify the quantum level and basis set effects. The CH stretching vibrations have values that are qualitatively different than those of the bends. The stretching modes are characterized by larger electron correlation treatment effects than basis set effects. Changing the quantum level from MP2 to QCISD can be up to ten times more effective than changing basis sets from 6-311G++(3d,3p) to cc-pVTZ. The bending vibrations have smaller effect values than the stretching ones and the electron correlation effects are similar in magnitude to the basis set ones. For all vibrations the interaction effects are small. So the effect of changing electron correlation treatment levels does not depend on the basis set used and *vice versa*. This means that a linear model relating the calculated intensities is an accurate

 This journal is © the Owner Societies 2014

Published on 25 September 2014. Downloaded by UNIVERSIDAD ESTADUAL DE CAMPINAS on 26/06/2015 20:14:22.

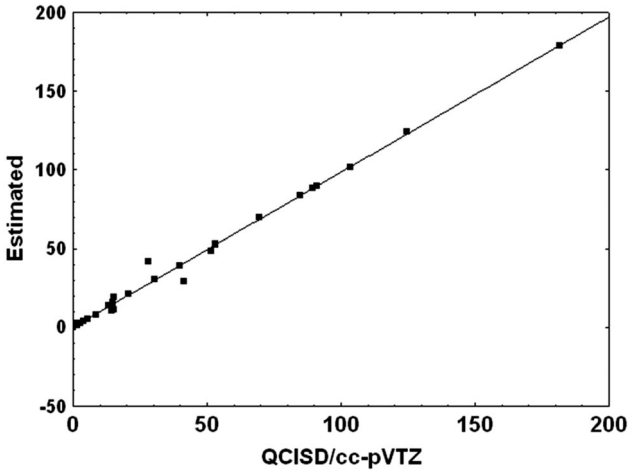

Fig. 2 Estimated hydrocarbon intensity values from QCISD/6-311++G(3d,3p), MP2/cc-pVTZ and MP2/6-311++G(3d,3p) results (eqn (4)) *vs.* calculated QCISD/cc-pVTZ values.

approximation. As such the intensities of all the normal modes are related by:

$$A_k(\text{QCISD/cc-pVTZ}) = A_k(\text{QCISD/6-311G++(3d,3p)}) - A_k(\text{MP2/6-311G++(3d,3p)}) + A_k(\text{MP2/cc-pVTZ}) \quad (4)$$

where A_k represents the intensity of the kth normal mode. The first two terms on the right hand side of this equation give the effect of changing the correlation electron level from MP2 to QCISD, which is added to the intensity directly calculated at the MP2 level with the Dunning basis set. The results are presented in the last column of Table 1 where they can be compared with the intensity values calculated with this basis but at the QCISD level. Fig. 2 shows that the correlation between the quantum and estimated values is exceptionally good, $r = 0.9968$. The rms error is only 3.3 km mol^{-1}.

Table 3 contains the QCISD/cc-pVTZ level charge, charge flux and dipole flux contributions as well as their interactions to the hydrocarbon intensities. Table S1 in the ESI† contains these results for all the calculations carried out in this work. Notice that the results in Table 3 for acetylene and propyne correspond to the results at the QCISD/6-311++G(3d,3p) level. Furthermore the CCFDF results for the total intensities of these two molecules have larger divergences from the intensities calculated directly from the molecular wave functions, rms error of 12.1 km mol^{-1} compared to 3.2 km mol^{-1} for intensities of the other molecules. The most pronounced deviations occur for Q_5 of acetylene and Q_9 of propyne with differences of 26 and 28 km mol^{-1}, respectively. Recently our laboratory has reported numerical problems using MORPHY98, caused mainly by difficulties integrating irregular atomic surfaces in carbon atoms surrounded by high electronic densities.[45]

Integration completely fails for acetylene and propyne when using the Dunning basis set. This problem for acetylene could be due to the existence of a (3,−3) critical point, usually associated with a nuclear critical point (or NCP), between the two carbon atoms. This critical point is not associated with any nucleus and, as such, is known as a non-nuclear attractor[11,46] or NNA. The MORPHY program is not designed to integrate electron density over the so-called non-nuclear attractors and even the integration over the other atoms that constitute the C_2H_2 molecule fail due to its presence. Some molecules with homopolar unsaturated bonds between two identical atoms have been reported to be more likely to indicate the presence of NNAs.[47–49] Acetylene (as Li_2, Na_2, P_2, S_2 and Si_2) is a well known example of this behavior when certain basis sets are employed in molecular calculations. Nonetheless there have been recent reports[47] suggesting that the presence of NNAs in heteronuclear molecules with similar electronegativities, such as in LiNa, are also favorable around their equilibrium geometries.

Discussion

Previous papers[13,14,50] on the QTAIM/CCFDF intensity models have reported strong negative correlations between charge flux and dipole flux contributions to dipole moment derivatives. This has been shown to be due to intramolecular charge transfer on vibrations accompanied by compensatory changes in electron density polarization adjusting to the new charge arrangement. Bader[10] has used this phenomenon of charge transfer-counter polarization to successfully explain the almost a null dipole moment of CO in spite of the fact that the electronegativity difference of its atoms implies that the oxygen atom is much more negatively charged than the carbon.

Charge transfer and counter polarization are accounted for by the second and third terms in eqn (2) for the dipole moment derivative. We have called these terms charge flux and dipole flux in line with the terminology from the older spectroscopic models. Their squares in eqn (3) provide contributions to the infrared intensities. The last term in eqn (3) is an interaction term that is the product of the charge flux and dipole flux dipole moment derivative contributions. If the equilibrium charge contribution is zero only the charge flux, dipole flux and their interaction term survive and their sum completely determines the intensity. For very polar bonds the first term can dominate the intensity although the fourth and fifth terms, the charge–charge flux and charge–dipole flux terms can be important. Most hydrogen atomic charges must be small since there have been many discussions about their signs in many molecules.[51,52] So one can expect the second, third and last terms in eqn (3) to be most important in the determination of the hydrocarbon CH intensities.

This is indeed the case. The charge flux contributions to the intensities range from zero to more than 1130 km mol^{-1} for the CH vibrations. The dipole flux has even higher values varying from 2 to 1750 km mol^{-1}. The charge term is normally much smaller than 10 km mol^{-1} except for the sp CH vibrations that range from 10 to 50 km mol^{-1}. The CH_2 rocking vibration for allene has a value within this interval, 17.4 km mol^{-1}.

The charge flux–dipole flux interaction contribution to the intensity, the last term in eqn (3), is negative because the

Published on 25 September 2014. Downloaded by UNIVERSIDAD ESTADUAL DE CAMPINAS on 26/06/2015 20:14:22.

Table 3 CCFDF contributions to the fundamental IR intensities of the hydrocarbons at the QCISD/cc-pVTZ level

Molecule	Q_j		C^2	CF^2	DF^2	C × CF	C × DF	CF × DF	Total
CH_4									
F_2	CH str	Q_3	0.06	902.3	1452.3	−15.0	19.1	−2289.5	69.3
F_2	CH bend	Q_4	0.1	81.5	220.1	5.9	−9.8	−267.8	30.0
C_2H_2									
Σ_u	CH str	Q_3	25.2	1785.0	1429.8	424.1	−379.4	−3194.0	90.7
Π_u	CH bend	Q_5	50.4	0.00	29.8	0.00	77.5	0.00	157.7
C_2H_4									
B_{1u}	CH_2 wag	Q_7	2.0	0.0	64.4	0.0	22.7	0.00	89.1
B_{2u}	CH_2 str	Q_9	1.5	774.0	1135.4	68.3	−82.7	−1874.9	21.6
	CH_2 rock	Q_{10}	0.5	14.1	6.8	−5.3	3.7	−19.5	0.3
B_{2u}	CH_2 str	Q_{11}	0.6	8.5	50.9	4.4	−10.8	−41.6	12.0
	CH_2 scis	Q_{12}	1.4	573.0	660.5	−57.3	61.6	−1230.5	8.7
C_2H_6									
A_{2u}	CH_2 str	Q_5	0.3	69.4	232.7	−9.3	17.0	−254.1	56.0
	CH_2 def	Q_6	1.9	225.4	310.2	41.9	−49.1	−528.8	1.5
E_u	CH_2 str	Q_7	2.1	1036.8	1750.7	−93.3	121.3	−2694.5	123.0
	CH_2 rock	Q_8	1.2	7.9	51.0	6.1	−15.4	−40.2	10.6
	CH_2 def	Q_9	1.2	42.6	108.0	14.6	−23.2	−135.6	7.6
C_3H_4 (propyne)									
	sp CH str	Q_1	9.5	1047.8	784.7	199.2	−172.4	−1813.5	55.3
	sp^3 CH str	Q_2	0.1	38.5	99.9	−2.8	4.5	−124.1	16.1
	C str	Q_3	2.9	9.7	0.0	−10.7	−0.5	0.9	2.3
	CH_3 bend	Q_4	0.3	155.8	142.9	14.5	−13.9	−298.2	1.4
	C–C str	Q_5	2.8	1.1	2.5	3.5	−5.3	−3.3	1.3
	sp^3 CH str	Q_6	0.4	629.6	788.2	−28.6	32.0	−1409.0	12.6
	CH_3 bend	Q_7	0.0	7.6	34.0	0.6	−1.4	−32.0	8.8
	CH_3 rock	Q_8	3.4	8.8	37.2	10.8	−22.4	−36.0	1.8
	CH bend	Q_9	19.0	0.0	13.2	−0.8	31.6	−0.6	62.4
	C–C bend	Q_{10}	7.2	0.2	2.6	2.4	8.8	1.4	22.6
C_3H_4 (allene)									
	CH str	Q_5	0.5	660.4	723.3	35.0	−36.8	−1379.0	3.4
	C═C str	Q_6	49.5	8519.5	6036.4	−1298.5	1093.0	−14342.2	57.7
	CH_2 bend	Q_7	10.3	447.5	434.2	−135.9	133.6	−880.0	9.7
	CH str	Q_8	3.0	697.0	907.6	91.6	−104.4	−1590.4	4.4
	CH_2 rock	Q_9	17.4	39.4	62.6	52.4	−66.0	−99.2	6.6
	CCC bend	Q_{10}	0.4	1.6	86.4	−0.2	10.8	−4.6	94.4
	CCC bend	Q_{11}	99.8	0.0	53.8	1.8	−146.6	−1.4	7.4
C_3H_6									
	CH str	Q_6	1.1	1138.2	1618.6	68.4	−81.6	−2714.6	30.1
	CH_2 rock	Q_7	0.4	32.4	27.3	−6.9	6.4	−59.4	0.0
	CH str	Q_8	0.4	227.9	494.4	19.7	−29.0	−671.3	42.1
	CH_2 def	Q_9	1.1	239.3	244.2	−32.0	32.3	−483.4	1.4
	CH_2 bend	Q_{10}	1.2	115.2	178.2	−23.9	29.7	−286.5	14.0
	Ring	Q_{11}	0.1	6.0	64.8	−1.0	3.7	−37.9	35.6

second and third dipole moment derivative terms in eqn (2) have opposite signs. Its values range from −2700 to zero km mol^{-1}. Finally the charge–charge flux and charge–dipole flux terms in eqn (3) have intermediate values between the pure charge and the flux terms.

Fig. 3 shows a graph of the sum of the charge flux and dipole flux intensity contributions against the charge flux–dipole flux interaction. As can be seen, the interaction contributions with negative signs almost perfectly cancel the charge flux and dipole flux sum. This cancellation is especially efficient for some of the CH stretching vibrations as the individual charge flux and dipole flux intensity contributions are so large. For example, the CH stretching of methane has charge and dipole flux contributions of 902.3 and 1452.3 km mol^{-1}. Summed with their interaction contribution of −2289.5 km mol^{-1} the net total is only 65.1 km mol^{-1}. This occurs even for the C═C stretching intensity of allene. The charge and dipole flux contributions are 8519.5 and 6036.4 km mol^{-1} whereas their interaction is −14342.2 km mol^{-1}. These very large, magnitude cancelling contributions are characteristic of all the quantum levels investigated here. For the CH stretch of methane the charge flux values range from 902.3 to 1141.2 km mol^{-1}, the dipole flux ones from 1440.8 to 1561.9 km mol^{-1} and their interaction values from −2670.2 to −2289.5 km mol^{-1} for these four calculation procedures. On the other hand their sums range from only 32.9 to 65.1 km mol^{-1}.

 This journal is © the Owner Societies 2014

Published on 25 September 2014. Downloaded by UNIVERSIDAD ESTADUAL DE CAMPINAS on 26/06/2015 20:14:22.

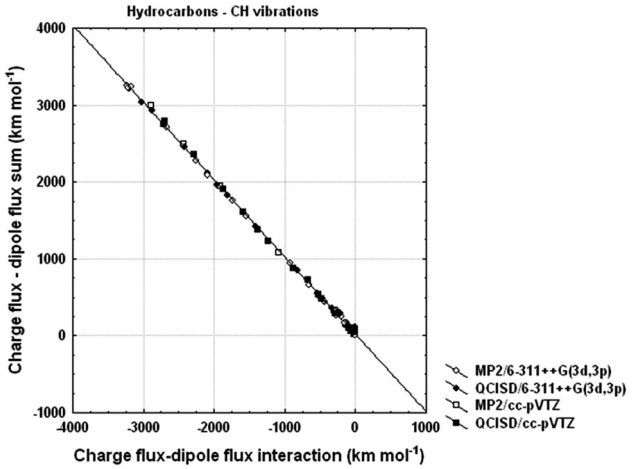

Fig. 3 Sum of charge flux and dipole flux intensity contributions *vs.* the charge flux–dipole flux interaction contribution.

The linear model regression results for the CH vibrations of all molecules at the calculation levels employed here (all CH vibrational results are provided in Table S1, ESI†) is

(Charge flux and dipole flux sum)

= 19.50 − 1.01 (Charge flux–dipole flux interaction)

with R^2 = 0.9994 and a standard error of only 3.23 km mol^{-1} and where the left side represents the sum of the second and third terms in eqn (3) and the factor on the right side is the last term in this equation. The very small intercept of 19.5 km mol^{-1} and slope close to unity are especially impressive considering the large range of more than 3000 km mol^{-1} for both the abscissa and ordinate.

With a negative correlation between the charge flux and dipole flux terms of the dipole moment derivative (eqn (2)) one anticipates an excellent negative correlation between the charge–charge flux and charge–dipole flux interaction intensity contributions (eqn (3)). This is shown in Fig. 4 where slight deviations from linearity are seen at the low and high ends of the ranges for these interaction values. This contributes to a regression slope of 1.000 and an intercept of 2.230 km mol^{-1}.

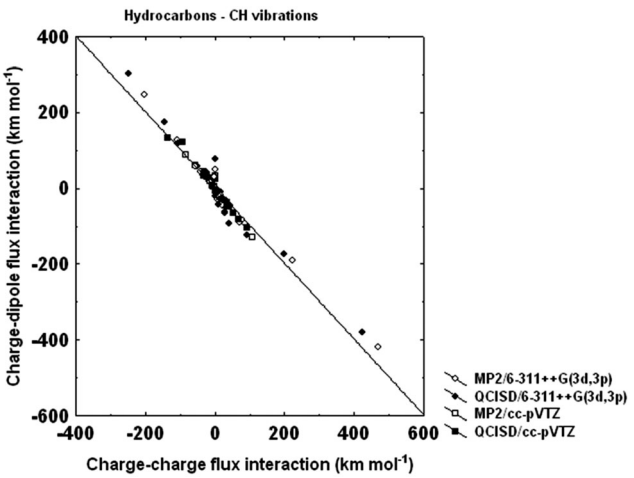

Fig. 4 The charge–charge flux interaction intensity contribution *vs.* the charge–charge flux interaction contribution.

(Charge–Dipole flux interaction)

= 2.23 − 1.00 (Charge–Charge Flux interaction)

with R^2 = 0.9531 and a standard error of 20.03 km mol^{-1} and where the left side is the second last term in eqn (3) and the factor on the right side is the fourth in this equation. Again, the graph in Fig. 4 includes the results from the use of both basis sets at each electron correlation treatment level. Even though

Table 4 Sums of the charge flux, dipole flux and their interaction, and the charge–charge flux and charge–dipole flux interactions as well as the sums of all five contributions and the total CCFDF intensity values

	$CF^2 + DF^2$ + 2CF × DF	2C × CF + 2C × DF	Sum	Intensity
CH_4				
Q_3	65.1	4.1	69.2	69.3
Q_4	33.8	−3.9	29.9	30.0
C_2H_2				
Q_3	20.8	44.7	65.5	90.7
Q_5	29.8	77.5	107.3	157.7
C_2H_4				
Q_7	64.4	22.7	87.1	89.1
Q_9	34.5	−14.4	20.1	21.6
Q_{10}	1.4	−1.6	−0.2	0.3
Q_{11}	17.8	−6.4	11.4	12.0
Q_{12}	3.0	4.3	7.3	8.7
C_2H_6				
Q_5	48.0	7.7	55.7	56.0
Q_6	6.8	−7.2	−0.4	1.5
Q_7	93.0	28.0	121.0	123.0
Q_8	18.8	−9.3	9.5	10.6
Q_9	15.0	−8.6	6.4	7.6
C_3H_4 (propyne)				
Q_1	19.0	26.8	45.8	55.3
Q_2	14.3	1.7	16.0	16.1
Q_3 (C str.)	10.6	−11.2	−0.6	2.3
Q_4	0.5	0.6	1.1	1.4
Q_5 (C–C str.)	0.3	−1.8	−1.5	1.3
Q_6	8.8	3.4	12.2	12.6
Q_7	9.6	−0.8	8.8	8.8
Q_8	10.0	−11.6	−1.6	1.8
Q_9	13.2	30.8	44.0	62.4
Q_{10} (C–C bend)	4.2	11.2	15.4	22.6
C_3H_4				
Q_5	4.7	−1.8	2.9	3.4
Q_6 (C═C str.)	213.7	−205.5	8.2	57.7
Q_7	1.7	−2.3	−0.6	9.7
Q_8	14.2	−12.8	1.4	4.4
Q_9	2.8	−13.6	−10.8	6.6
Q_{10} (C–C–C bend)	83.4	10.6	94.0	94.4
Q_{11} (C–C–C bend)	52.4	−144.8	−92.4	7.4
C_3H_6				
Q_6	42.2	−13.2	29.0	30.1
Q_7	0.3	−0.5	−0.2	0.2
Q_8	51.0	−9.3	41.7	42.1
Q_9	0.1	0.3	0.4	1.5
Q_{10}	6.9	5.8	12.7	13.9
Q_{11} (ring)	32.9	2.7	35.6	40.3

Published on 25 September 2014. Downloaded by UNIVERSIDAD ESTADUAL DE CAMPINAS on 26/06/2015 20:14:22.

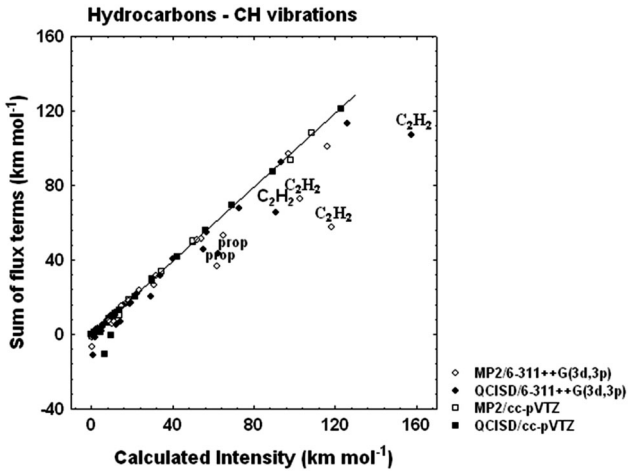

Fig. 5 The sum of the charge flux, dipole flux, charge–charge flux, charge dipole flux and charge flux–dipole flux contributions to the intensity *vs.* calculated CCFDF intensity values.

the charge flux and dipole flux derivative terms can be large the charge–charge flux and charge–dipole flux intensity contributions are modulated by the small equilibrium charges of the hydrogen atoms in these hydrocarbons. In almost all cases these intensity contributions have opposite signs and tend to cancel one another. These interaction contributions can be positive or negative. Of the 30 CH vibrations listed in Table 3 about half have positive charge–charge flux interactions. All of these positive charge–charge flux contributions are accompanied by negative charge–dipole flux contributions except one, a C–C bending mode in propyne that has a small value, 2.4 km mol^{-1}.

Since the sum of the charge flux and dipole flux intensity contributions is so highly correlated with the charge flux–dipole flux interactions one expects their sums to be small for all the CH vibrations investigated here. This is indeed true as can be seen in Table 4. Its first numerical column contains these sum values ranging from about zero to 93 km mol^{-1}, which are much smaller than the values of the individual contributions that range from zero to several thousand km mol^{-1}. The same holds for the sum of the charge–charge flux and charge–dipole flux contributions that range from close to zero to a little above 100 km mol^{-1} whose values are listed in the second column of the table.

The second last column in Table 4 contains a sum of the values in the first two columns, *i.e.* it is a sum of all contributions to the hydrocarbon intensities except the charge. These values for all the CH vibrations, whether they are stretching, bending, deformation, *etc.* are in excellent agreement with the total intensity values. The rms errors are very small for all calculational levels being 11.6 km mol^{-1} for the QCISD/cc-pVTZ results. A plot of the sums of all terms involving flux against the total calculated intensity is shown in Fig. 5. Almost all the points are on or close to the line representing exact agreement. The notable exceptions are the four points for the CH stretching and bending intensities of acetylene calculated using the 6-311++G(3d,3p) basis set at the MP2 and QCISD levels. These deviations can be explained by their high charge contributions, 25.2 and 50.4 km mol^{-1} (QCISD/6-311++G(3d,3p) level), for the stretching and bending vibrations, respectively. Smaller deviations occur for the Q_1 and Q_9 intensities of propyne that have charge contributions of 9.5 and 19.0 km mol^{-1} at the QCISD/cc-pVTZ level. These vibrations are the sp CH stretching and bending motions as might be expected. Removing the vibrations involving the two acetylene and two propyne vibrations reduces the rms error to only 4.2 km mol^{-1}, which is quite low considering that the calculated intensities range from 0.3 to 123.0 km mol^{-1}.

Fig. 6 contains a graph comparing the charge intensity contributions (lower line) with the sum of the other five terms involving the charge and/or dipole flux contributions (middle line). Their sum is represented by the upper solid line in the graph. Only two acetylene, two propyne and two allene vibrations have charge intensity contributions noticeably different from zero. The lines representing the sum of only the flux terms are almost identical to the lines for the total calculated values of all the other intensities except for these six.

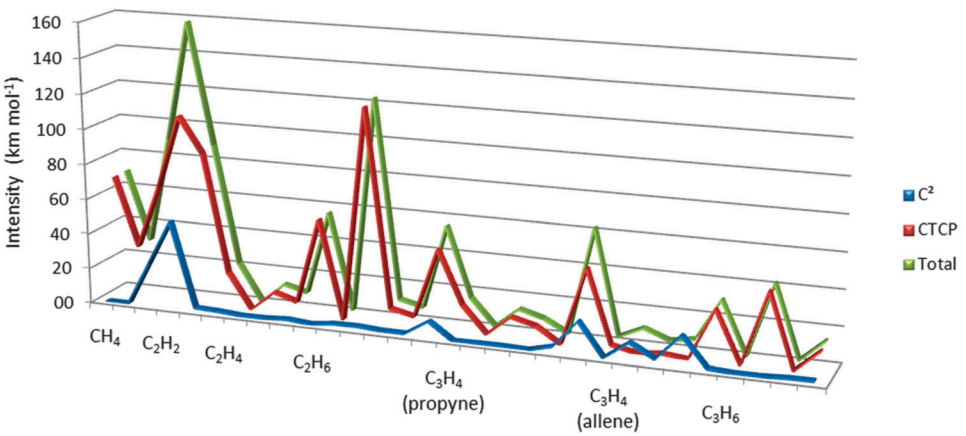

Fig. 6 Graphs of the charge contribution, the contributions owing to all terms with flux factors and the total calculated intensities for the simple hydrocarbons.

 This journal is © the Owner Societies 2014

Published on 25 September 2014. Downloaded by UNIVERSIDAD ESTADUAL DE CAMPINAS on 26/06/2015 20:14:22.

These results provide clear evidence that only the charge transfer-counter polarization effect is necessary to quantitatively determine the CH stretching and bending intensity values of hydrocarbons involving sp^3 and probably most sp^2 hybridized carbon atoms. For acetylene and the other vibrations involving sp hybridized carbon atoms equilibrium charge contributions need to be added to other terms involving charge transfer and counter polarization.

Charge transfer-counter polarization effects are probably important to describe electronic density changes accompanying vibrations in general. One of our previous studies[14] showed that the fundamental intensities of the CF stretching modes can be calculated from the charge, charge–charge flux and charge–dipole flux contributions, *i.e.* the first, fourth and fifth terms in eqn (3). As the fluorine equilibrium charge is large owing to its electronegativity these terms are much larger than the other three that do not contain a charge factor. Intensity values for 20 CF stretching vibrations of the difluoroethylenes, the fluoro- and fluorochloromethanes, F_2CO and F_2CS were calculated with a 32 km mol^{-1} rms error. This is quite good as the average intensity of these vibrations was 195 km mol^{-1} and the individual values ranged from 4 to 470 km mol^{-1}.

Conclusion

The charge transfer-counter polarization effect was proposed some years ago by Bader to explain the almost null dipole moment of CO. The dipole moment contribution owing to charge transfer from carbon to oxygen on bond formation is compensated by electron density polarizations in the opposite direction. Here, this phenomenon has been employed to accurately determine 30 infrared CH stretching, bending and deformation intensities for molecules with sp^3 and sp^2 carbon atoms. Equilibrium charge considerations must also be taken into account for describing intensities involving hydrogens bonded to sp carbons but the charge transfer-counter polarization effect is still important for their vibrations. In fact this effect seems to be important for most vibrations although the equilibrium charge could be the dominating contribution as for the CF stretching intensities. In fact the large dipole moment derivative of CO itself can only be explained by a combination of equilibrium charge and the charge transfer-counterpolarization effects. Since the charge transfer-counter polarization effect is by far the dominant one for quantitatively explaining the infrared intensites of the CH bond vibrations it can be expected to be important for explaining more complicated phenomena such as chemical reactivity where bond distortions are much more pronounced.

Acknowledgements

W.E.R. and A.F.S. thank CNPq (Conselho Nacional de Desenvolvimento Científico e Tecnológico grants 140916/2011-3 and 140711/2013-9) for graduate student fellowships and R.E.B. thanks CNPq for a research fellowship. We are also grateful to FAPESP (Fundação de Amparo à Pesquisa do Estado de São Paulo) for partial financial support of this work (grant 09/09678-4).

References

1 W. T. King, G. B. Mast and P. P. Blanchette, *J. Chem. Phys.*, 1972, **56**, 4440.
2 L. A. Gribov, *Intensity Theory for Infrared Spectra of Polyatomic Molecules*, Consultants Bureau, N. Y., 1964.
3 J. C. Decius, *J. Mol. Spectrosc.*, 1975, **57**, 348.
4 A. J. Straten and W. M. A. Smit, *J. Mol. Spectrosc.*, 1976, **62**, 297.
5 M. Gussoni, P. Jona and G. Zerbi, *J. Chem. Phys.*, 1983, **78**, 6802.
6 M. Gussoni, M. N. Ramos, C. Castiglioni and G. Zerbi, *Chem. Phys. Lett.*, 1987, **142**, 515.
7 M. Gussoni, M. N. Ramos, C. Castiglioni and G. Zerbi, *Chem. Phys. Lett.*, 1989, **160**, 200.
8 A. Milani and C. Castiglioni, *J. Phys. Chem. A*, 2010, **114**, 624.
9 W. T. King and G. B. Mast, *J. Phys. Chem.*, 1979, **80**, 2521.
10 R. F. W. Bader and C. F. Matta, *J. Phys. Chem. A*, 2004, **108**, 8385.
11 R. F. W. Bader, *Atoms in Molecules: A Quantum Theory*, Clarendon Press, Oxford, 1990.
12 R. F. W. Bader, A. Larouche, C. Gatti, M. T. Carrol, P. J. MacDougall and K. B. Wiberg, *J. Chem. Phys.*, 1987, **87**, 1142.
13 R. L. A. Haiduke and R. E. Bruns, *J. Phys. Chem. A*, 2005, **109**, 2680.
14 A. F. Silva, W. E. Richter, H. G. C. Meneses, S. H. D. M. Faria and R. E. Bruns, *J. Phys. Chem. A*, 2012, **116**, 8238.
15 E. B. Wilson and A. J. Wells, *J. Chem. Phys.*, 1946, **14**, 578.
16 S. S. Penner and D. Weber, *J. Chem. Phys.*, 1951, **19**, 807.
17 B. L. Crawford, Jr., *J. Chem. Phys.*, 1952, **20**, 977.
18 W. B. Person and J. H. Newton, *J. Chem. Phys.*, 1974, **61**, 1040.
19 J. F. Biarge, J. Herranz and J. Morcillo, *An. R. Soc. Esp. Fis. Quim., Ser. A*, 1961, **57**, 81.
20 J. A. Pople, M. Head-Gordon and K. Raghavachari, *J. Chem. Phys.*, 1987, **87**, 5968.
21 A. Szabo and N. S. Ostlund, *Modern Quantum Chemistry*, Dover Publications, Inc., New York, 1982.
22 F. Jensen, *Introduction to Computational Chemistry*, John Wiley and Sons, 2nd edn, 2007.
23 B. Galabov, Y. Yamaguchi, R. B. Remington and H. F. Schaefer III, *J. Phys. Chem. A*, 2002, **106**, 819.
24 J. V. da Silva, Jr., L. N. Vidal, P. A. M. Vazquez and R. E. Bruns, *Int. J. Quantum Chem.*, 2010, **110**, 2029.
25 A. E. Oliveira, R. L. A. Haiduke and R. E. Bruns, *J. Phys. Chem. A*, 2000, **104**, 5320.
26 M. J. Frisch, G. W. Trucks, H. B. Schlegel, G. E. Scuseria, M. A. Robb, J. R. Cheeseman, J. A. Montgomery Jr., T. Vreven, K. N. Kudin, J. C. Burant, J. M. Millam, S. S. Iyengar, J. Tomasi, V. Barone, B. Mennucci, M. Cossi, G. Scalmani, N. Rega, G. A. Petersson, H. Nakatsuji, M. Hada, M. Ehara, K. Toyota, R. Fukuda, J. Hasegawa, M. Ishida, T. Nakajima, Y. Honda, O. Kitao, H. Nakai, M. Klene, X. Li, J. E. Knox, H. P. Hratchian, J. B. Cross, V. Bakken, C. Adamo, J. Jaramillo, R. Gomperts, R. E. Stratmann, O. Yazyev, A. J. Austin, R. Cammi, C. Pomelli, J. W. Ochterski, P. Y. Ayala, K. Morokuma, G. A. Voth, P. Salvador, J. J. Dannenberg, V. G. Zakrzewski, S. Dapprich, A. D. Daniels, M. C. Strain, O. Farkas, D. K. Malick, A. D. Rabuck, K. Raghavachari, J. B. Foresman, J. V. Ortiz, Q. Cui,

Published on 25 September 2014. Downloaded by UNIVERSIDAD ESTADUAL DE CAMPINAS on 26/06/2015 20:14:22.

A. G. Baboul, S. Clifford, J. Cioslowski, B. B. Stefanov, G. Liu, A. Liashenko, P. Piskorz, I. Komaromi, R. L. Martin, D. J. Fox, T. Keith, M. A. Al-Laham, C. Y. Peng, A. Nanayakkara, M. Challacombe, P. M. W. Gill, B. G. Johnson, W. Chen, M. W. Wong, C. Gonzalez and J. A. Pople, *Gaussian 03, Revision D.02*, Gaussian, Inc., Wallington CT, 2004.

27 MORPHY98, a program written by P. L. A. Popelier with a contribution from R. G. A. Bone, UMIST, Manchester, England, EU, 1998.

28 T. C. F. Gomes, J. V. Silva, Jr., L. N. Vidal, P. A. M. Vazquez and R. E. Bruns, *Quim. Nova*, 2008, **31**, 1750.

29 J. H. G. Bode and W. M. A. Smit, *J. Phys. Chem.*, 1980, **84**, 198.

30 S. Saëki, M. Mizuno and S. Kondo, *Spectrochim. Acta, Part A*, 1976, **32**, 403.

31 K. Kim, *J. Quant. Spectrosc. Radiat. Transfer*, 1987, **37**, 107.

32 D. F. Eggers, R. Rollefson and B. S. Schurin, *J. Chem. Phys.*, 1951, **19**, 1595.

33 K. Kim and W. T. King, *J. Mol. Struct.*, 1979, **57**, 201.

34 T. Koops, W. M. A. Smit and T. Visser, *J. Mol. Struct.*, 1984, **112**, 285.

35 R. C. Golike, I. M. Mills, W. B. Person and B. L. Crawford, Jr., *J. Chem. Phys.*, 1956, **25**, 1266.

36 T. Nakanaga, S. Kondo and S. Saeki, *J. Chem. Phys.*, 1979, **70**, 2471.

37 J. H. G. Bode, W. M. A. Smit, T. Visser and H. D. Verkruisse, *J. Chem. Phys.*, 1980, **72**, 6560.

38 S. Kondo and Y. Koga, *J. Chem. Phys.*, 1978, **69**, 4022.

39 I. M. Nyquist, I. M. Mills, W. B. Person and B. L. Crawford, Jr., *J. Chem. Phys.*, 1957, **26**, 552.

40 Y. Koga, S. Kondo, T. Nakanaga and S. Saëki, *J. Chem. Phys.*, 1979, **71**, 2404.

41 I. W. Levin and R. A. R. Pearce, *J. Chem. Phys.*, 1978, **69**, 2196.

42 J. Overend, in *Infrared Spectroscopy and Molecular Structure*, ed. M. Davies, Elsevier, Amsterdam, 1963.

43 A. E. Oliveira, R. L. A. Haiduke and R. E. Bruns, *J. Phys. Chem.*, 2000, **104**, 5320.

44 R. E. Bruns, I. S. Scarminio and B. de Barros Neto, *Statistical Design – Chemometrics*, Elsevier, Amsterdam, 2006.

45 A. F. Silva, J. V. da Silva, Jr., R. L. A. Haiduke and R. E. Bruns, *J. Phys. Chem. A*, 2011, **115**, 12572.

46 M. Pandás, M. A. Blanco, A. Costales, P. M. Sánchez and V. Luaña, *Phys. Rev. Lett.*, 1999, **83**, 1930.

47 R. D. Alcoba, L. Lain, A. Torre and C. R. Bochicchio, *Chem. Phys. Lett.*, 2005, **407**, 379.

48 L. A. Terrabuio, T. Q. Teodoro, M. G. Rachid and R. L. A. Haiduke, *J. Phys. Chem. A*, 2013, **117**, 10489.

49 V. Tognetti and L. Joubert, *J. Phys. Chem. A*, 2011, 5505A.

50 A. F. Silva, W. E. Richter, L. A. Terrabuio, R. L. A. Haiduke and R. E. Bruns, *J. Chem. Phys.*, 2014, **140**, 084306.

51 K. B. Wiberg and P. R. Rablen, *J. Comput. Chem.*, 1993, **14**, 1504.

52 K. B. Wiberg and J. J. Wendoloski, *J. Phys. Chem.*, 1984, **88**, 586.

 This journal is © the Owner Societies 2014